



Vacuum insulated glazing (VIG) units under wind load—part 1: global deformation and stresses on the outer glass surfaces

Isabell Ayvaz · Cenk Kocer · Jens Schneider

Received: 1 March 2023 / Accepted: 25 October 2023 / Published online: 23 November 2023
© The Author(s) 2023

Abstract This paper presents the first part of a study on the effect of wind loads on Vacuum Insulated Glass (VIG) units. The study provides background information on VIG and relevant Standards, explains the numerical modelling process, and discusses the implications of the results in relation to European and North American codes and Standards. The focus of the study is on vertical windows and façade installations in low-rise buildings (< 25 m) commonly found in residential buildings. The mechanical behaviour of VIG was analysed using the Finite Element Method (FEM) with respect to various design parameters such as glass pane size, glass thickness, surface pressure magnitude, and edge boundary conditions. The study analysed global deformation as well as the stresses on the outer glass surfaces. The VIG features such as pillar geometry and contact dynamics, and material non-linear effects, were explicitly modelled. In addition, monolithic glass plates were also modelled, and the FEM results of the monolithic cases were in reasonable agreement with an analytical solution obtained from linear thin

plate theory. These results highlight the limit of linear behaviour in monolithic plate bending. The centre-of-pane deflection of the VIG was in good agreement with the FEM and analytical solutions of the equivalent thickness monolithic pane, for sample sizes below 800 × 800 mm. However, for larger glass sizes, a deviation was found, and the VIG exhibited a higher plate stiffness than the equivalent thickness monolithic pane. The simulations also showed that the stresses in the glass panes are highly dependent on the edge of glass boundary condition. Finally, the results demonstrated that with appropriate design choices, the VIG can satisfy the Standards requirements for wind load and glass design in both Europe and North America.

Keywords Vacuum insulated glazing · Wind load · Design criteria

1 Introduction

The use of Vacuum Insulated Glazing (VIG) has gained increasing interest among architects and engineers seeking to design energy-efficient building envelopes. While this technology has been widely adopted in Asian markets since the late 1990s, there has been a growing interest in North America and Europe due to advancements in government environment policies and building codes. As a result, commercial entities in these regions are developing VIG products and working towards high-volume manufacturing in the near future.

I. Ayvaz (✉) · J. Schneider
Glass Competence Center, Institute of Structural Mechanics and Design, TU Darmstadt, Darmstadt, Germany
e-mail: ayvaz@ismd.tu-darmstadt.de

J. Schneider
e-mail: schneider@ismd.tu-darmstadt.de

C. Kocer
School of Physics, University of Sydney, Sydney, Australia
e-mail: cenk.kocer@sydney.edu.au

However, the current lack of national Standards that harmonize VIG design means that the installation of VIGs in buildings in Europe or North America requires the design of the VIG product to satisfy case-by-case building specific approvals (Schulz et al 2023). Only the ISO Standard 19916-1 (2018) and 19916-3 (2021) are currently available that were explicitly proposed for VIG design. Yet, these two Standards only provide guidance on acoustic performance, U-value measurements, vacuum stability tests, and thermal load performance. Guidance with respect to mechanical performance and testing under wind load has not been released.

While the thermal performance of a VIG, as well as its mechanical performance under the permanent strain of atmospheric pressure, is well published (Collins et al 1999; Collins and Robinson 1991; Collins et al. 1993; Turner et al. 1994; Fischer-Cripps et al. 1995; Fang et al. 2007; Ng et al. 2007; Aronson and Kocer 2017), there are few publications that discuss wind load effects on a VIG unit. To the best of our knowledge, only Liu and Bao (2013) and Schulz et al. (2023) have studied the VIG under a surface pressure (representing the effects of wind loads as stipulated in the Standards (compare Sect. 4)), by performing physical measurements. Chiu (2015) studied the effects of a static, and dynamic, point load on a VIG, through measurements and finite element modeling at the University of Sydney. The studies suggest that the VIG, as a coupled pair of glass sheets, can be replaced by an equivalent monolithic thickness that is about 85–95% of the total thickness of the VIG panes. Unfortunately, the studies are limited and consider only a small set of parameters; for example, Liu et al. only consider two pane sizes (300 × 300 mm and 1000 × 1000 mm), a single edge boundary condition, which is not explicitly tracked (e.g. by measuring whether the pane can move within the frame) so that comparison with idealized FEM data is difficult. In addition, only data (strains and deflection) at the centre of the glass panes are provided. No information about deformation and stress results over the surface, neither clearly adoptable edge boundary conditions are described.

The aim of this paper is to investigate the effects of wind load on a VIG unit, specifically on the overall deformations of the glass panes and the stress distribution throughout the panes. To achieve this, the finite element method (FEM) was used to analyze several design parameters that affect the mechanical behavior of a VIG

when subjected to a surface pressure, which is within the range of pressures stated in relevant EU and North American Standards. The study focuses on the impact of glass pane size, glass thickness, the magnitude of the surface pressure, and the edge boundary conditions. The goal is to design a VIG that satisfies the requirements of existing wind Standards and glass codes while providing the benefits of decreased U-values and a thin profile. The paper begins with a description of the relevant background of VIG in Sect. 2, followed by a brief review of relevant Standards in Sect. 3, which includes the defined scope of buildings concerning location. The Standards EN 16612 (2019–12) and ASTM E1300-16 (2016) were applied to define the resistance side (glass strength), and ASCE 7–16 (2016) and EN 1991-1-4:2005/AC:2010 (2010) were taken into consideration to define the wind load side. The approach taken here is limited to vertical windows and façade installations typical in low rise buildings (buildings < 25 m according to EN 1991-1-4 2010), which covers the majority of window applications in residential buildings. In Sect. 4, the numerical modelling of the VIG and the relevant parameters employed in this work are outlined. In a final step (Sect. 6), the implications of the results are discussed in relation to the considered codes and Standards.

2 The vacuum insulated glazing

The stresses produced in a VIG unit under external loads are not trivial, and more complex than that produced in single glass panes. Figure 1 illustrates the typical construction of a VIG unit. Similar to the gas-filled Insulated Glazing Units (IGU), the VIG consists of at least two panes of glass that are separated by a gap, which provides the thermal insulation between the inside and outside environments. However, unlike in an IGU, the gap in the VIG is evacuated to a pressure of about 0.001 Torr (0.1 Pa), which reduces gaseous conduction and convection to a negligible level (Collins and Fischer-Cripps 1991). The gap size is in a range of 0.1–0.3 mm, making the VIG a slender yet highly energy-efficient window unit (Schulz et al. 2022). In general, a single pane of glass has an air-to-air U-value of about $5.8 \text{ W m}^{-2} \text{ K}^{-1}$, existing IGUs can typically be as low as $0.6 \text{ W m}^{-2} \text{ K}^{-1}$, while the VIGs can reach U-values as low as $0.3 \text{ W m}^{-2} \text{ K}^{-1}$ (Kocer 2011, 2013; Lee et al. 2018; Park et al. 2019). Besides, VIG products

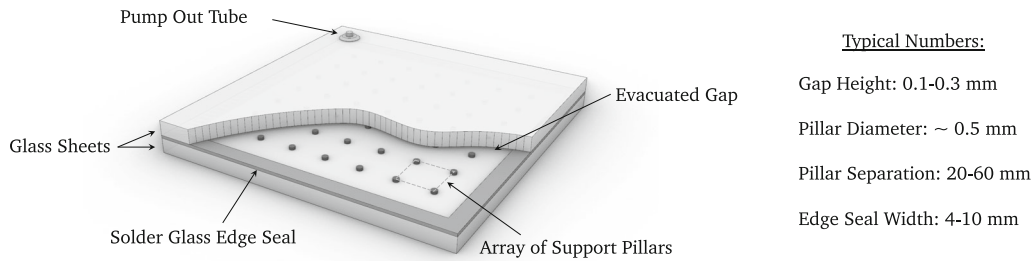


Fig. 1 An illustration of the VIG unit construction. On the right are typical values for the primary parameters

available today can be adapted to the specific requirements of building projects; for example, using annealed and tempered glass, integrating the VIG in the setup of gas filled IGUs (known as the 'Hybrid VIG' (Schulz et al 2023)) or laminating the VIG to a monolithic pane. To provide vacuum stability over a service life of at least 25 years, VIGs are hermetically sealed around their perimeter. The hermetic edge is currently either made from solder glass (a type of glass frit) or a metal solder (e.g. Indium solder).

Over its lifetime the VIG must permanently withstand the strain of atmospheric pressure, which results from the evacuation of the gap and is about 100,000 Pa (representing a mass equivalent of 10 tons per m²). An array of spacers (also known as pillars) is placed between the panes to maintain separation under atmospheric pressure (source: Riedel et al. 2022). Typically, the pillars are made from high-strength metal alloys that can withstand the high compressive stress due to atmospheric pressure: a compressive strength greater than 1 GPa (Collins and Fischer-Cripps 1991) and are usually arranged as a square array.

The glass areas in a VIG that will experience tensile stresses, which are typically critical in glass design (Collins and Fischer-Cripps 1991), are well-defined (Turner et al. 1994):

1. Bending of the unsupported glass between and above the pillars, where the tensile stress is over areas directly above the pillars over the external surfaces and in between pillars over the internal vacuum side surfaces,
2. Bending of the unsupported glass between the edge seal and the pillars, where the tensile stresses are on the external and internal glass surfaces, and,

3. Indentation due to contact between the pillars and the glass surface, which produces high gradient tensile stresses on the glass surface near the glass-pillar contact area on the internal vacuum side surfaces.

The resulting bending tensile stresses due to atmospheric pressure are permanently present in a VIG and must therefore always be superimposed with resulting stresses from other effects. Wind, in particular, causes additional bending tensile stresses, which must be combined with those from atmospheric pressure.

Published works in the literature provide insight into the magnitude and distribution of stress that would be experienced in a VIG due to atmospheric pressure (e.g., Collins and Fischer-Cripps 1991, Turner et al. 1994). There are two regions that are of most interest because of the higher tensile stresses that result, and where the higher fracture probability is found. Firstly, is the tensile stress over the external glass surfaces above pillars, where the maximum tensile stress is dependent on the separation between the pillars and the thickness of the glass panes (see Fig. 2) because of the bending of the glass over the pillars. Secondly, the maximum tensile stress at the glass-to-pillar contact on the internal glass surfaces. The probability of failure in these two regions are found to be different because of the difference in the distribution of the tensile stress and the effect of the vacuum environment. It is found that the probability of failure is higher on the external glass surfaces, and therefore, the glass thickness and the spacing of the pillar array are critical parameters in the design of the VIG, with respect to atmospheric forces (Collins and Fischer-Cripps 1994).

Moreover, the extension of cracks through soda-lime glass is well-known to originate from surface flaws

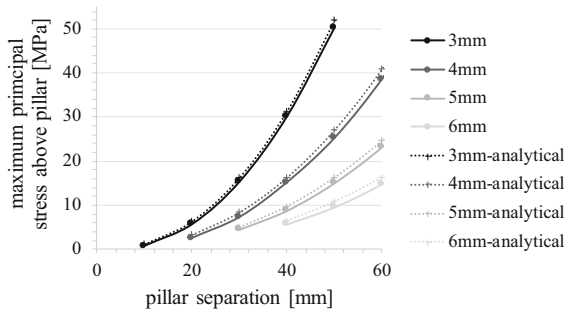


Fig. 2 Comparison of the maximum principal stress on the outer glass surface above the pillars, as a function of the pillar separation; solid lines are numerical calculations obtained by a unit cell model and dashed lines are analytical solutions (compare Colins and Fischer-Cripps 1991)

(Griffith 1921), which on the one hand need to be favorably located and oriented to induce fracture (Schneider et al. 2016). On the other hand, their propagation exhibits a high dependency on the level of moisture in the environment (Budd 1961; Michalske and Freiman 1982, 1983; Meyland et al 2021). This is why, it is reasonable to assume that the probability of failure will always be higher on the external surfaces exposed to the environment when compared directly to the probability of glass fracture within the vacuum gap (Fischer-Cripps et al. 1995), for an equivalent stress field. In this work the focus is therefore on the tensile stresses that are created on the external surfaces of the glass panes. The full effect of the pillar-to-glass contact is a focus of on-going research which will be published as the sequel to this paper.

3 Wind loading on glass components: a building code and standards perspective

The design of façade components requires engineers to ensure that the defined limits for mechanical stresses, as well as deformations, are not exceeded in the window or its supporting structure. As no normative specifications are currently available for a VIG, which allow it to be designed for wind loads, in this section we review the relevant requirements as outlined in the American Society of Civil Engineers code (ASCE 7–16) and Eurocode 1 (EN 1991-1-4:2010) on the action side as well as ASTM E1300 ‘Standard Practice for Determining Load Resistance of Glass in Buildings’ and EN 16612:2019 ‘Glass in building—Determination of the

lateral load resistance of glass panes by calculation’ on the load resistance side.

According to Eurocode 1 (EN 1991-1-4:2010), wind actions are defined as variable free actions that fluctuate with time. To simplify the analysis process, wind action as defined in the Standards are typically a quasi-static pressure, which defined an equivalent response with respect to the extreme effects of fluctuating wind loads (Holmes 2007). Gavanski and Kopp (2011) show that, in general, this is appropriate for most, if not all, glass structures. Their experiments indicate that damage accumulation, which can lead to failure of glass components, is not dependent on the load profile. Thus, in this work the VIG is subjected to a static surface pressure as an equivalent wind load. The equivalent surface pressure employed in this work for a wind load was determined using the wind pressure limits as defined for low rise buildings (including buildings < 25 m (Europe), < 18 m (USA)). The maximum wind pressure limit considered in this study was calculated from the data, and procedures, outlined in the EN 1991-1-4:2010 and ASCE 7–16 documents, which is a maximum design wind load of 2 kPa, and is the upper limit used in this study. The wind speed used to determine the maximum wind load includes the majority of the façade area (building corners are excluded) in urban regions and was chosen so that it includes 95% of wind zones in the USA and Europe (according to existing wind hazard maps in the Standards). Only rigid building components were considered, i.e. dynamic effects were neglected. Risk category 2 (compare ASCE 7) was considered. The factors required in EN 1991-1-4:2010 accounting for direction (c_{dir}) and seasonal influences (c_{season}) as well as the coefficients accounting for roughness ($c_r(z)$) and topography ($c_0(z)$) were set to 1.0. The exposure coefficient c_e was determined according to EN 1991-1-4:2010 figure 4.2. In the American equivalent, the topographic factor K_{zt} and ground elevation factor K_e were set to 1.0 and the wind directionality factor K_d was set to 0.85. The combined gust load factor and external pressure coefficient GC_p was determined according to ASCE-7–16 figure 30.3–1. The wind load duration used to determine the maximum wind load was the 10-min averaging time in Europe and 3 s gust wind load in the US. Coincidentally, in both cases, it resulted in a maximum wind load of 2 kPa for the considered locations and building types.

In order to establish appropriate design limits for the VIG structure, it is crucial to understand how wind behaves and how it relates to the underlying strength of the glass panes. In North America, the ASTM E1300 (2016) provides guidance on how to design glass structures. For an independent stress analysis, Annex X6 specifies the maximum allowable surface stresses for different types of glass, based on a 3-s load duration. This load duration was also used to determine the maximum load on the action side. The design strength for annealed glass (AN) is 23.3 MPa, while for fully tempered glass (FT), it is 93.1 MPa. On the other hand, the European Standard EN 16612:2019 provides the characteristic bending strength of annealed glass and fully tempered glass as 45 MPa and 120 MPa, respectively. The partial safety factor $\gamma_{M,a}$ for AN and $\gamma_{M,y}$ for FT glass are 1.8 and 1.2, respectively. Using these values, the design strength limit for a 10-min load duration (which is the wind load averaging time according to EN 1991-1-4:2010 and also used to determine the maximum load on the action side) is 18.5 MPa for AN and 81.0 MPa for FT. These values will be used as an acceptable stress limit in the discussion in Sect. 5.

Now that the strength limits are clearly defined from the two Standards, it is a matter of determining the limits of the design parameters with respect to the allowable maximum tensile stress in the glass (Fischer-Cripps and Collins 1995). In the following section, the finite element modelling of a VIG subjected to a constant surface pressure is presented.

4 The numerical model

In this study, we focused on the traditional design of VIG in our simulations, which consists of the following characteristics:

1. The VIG comprises two glass panes of equal thickness, which are square in shape.
2. A rigid solder glass of defined width is used as the perimeter edge seal.
3. The cylindrical pillars are made of metal and are positioned as a regular square array within the vacuum gap.

To conduct the simulations, we employed FEM software ANSYS 18.0. In all FEM simulations, we fully replicated the VIG device, including its geometry and material properties such as the glass panes, the rigid

edge seal, and the cylindrical pillars. We also accounted for the effects of large deformations and non-linear material behaviour.

In the FEM model element types SOLID185/SOLID186 were employed, along with the CONTA174 and TARGE170 elements, to represent all of the geometric and load configurations, boundary/constraint conditions, non-linear effects, as well as, the pillar-to-glass contact. The mesh density of the models was optimized, in particular, in areas of high stress gradients, i.e., around the pillar contact and the edge of glass. The mesh size in the model varied from 0.01 to 2 mm, and provided convergence and stability while minimizing the required computing resources. An illustration of the different mesh regions in the FE model are given in Fig. 3. The Ansys Parametric Design Language (APDL) was used to perform the parametric study that provided data over a large parameter space. All solutions were obtained on a High-Performance Computing (HPC) cluster, with 7,636 cores (CPUs), 45 TB of RAM, 378 TB of storage and on 56 Gbps FDR InfiniBand network.

In the model the advantage of mirror symmetry, in-plane of the glass, was used, i.e. only a quarter of the VIG unit was modelled, as highlighted in Fig. 4. Simplifying the model in this way significantly reduces the computing time and the size of the data files. In Fig. 4 the edge-to-centre is highlighted, over which the surface stress, and deformation, data were determined; these data are presented in Sect. 6.

To define the glass-metal contact surface, the CONTA174-TARGE170 element pair was used, with a coefficient of static friction of 0.9 representing the expected high contact friction between the metal and glass in the dry vacuum environment. Two edge constraints were modeled to represent the potential extremes of the constraint due to a window frame. The first constraint, referred to as BC 1, was "simply supported," meaning that the element nodes over all four glass edges were fixed in the z-direction only, and rotation at the nodes was allowed. The second, referred to as BC 2, was the "fixed" case, where the element nodes over a width of 10 mm at the glass edge were fixed in all directions on the glass surface, and rotation of the nodes was not allowed. While BC 2 does not represent a "real" framing configuration, it is reproducible in experiments, and the measured mechanical behavior of the VIG unit is found to be in good agreement with the results observed in FEM simulations. This was

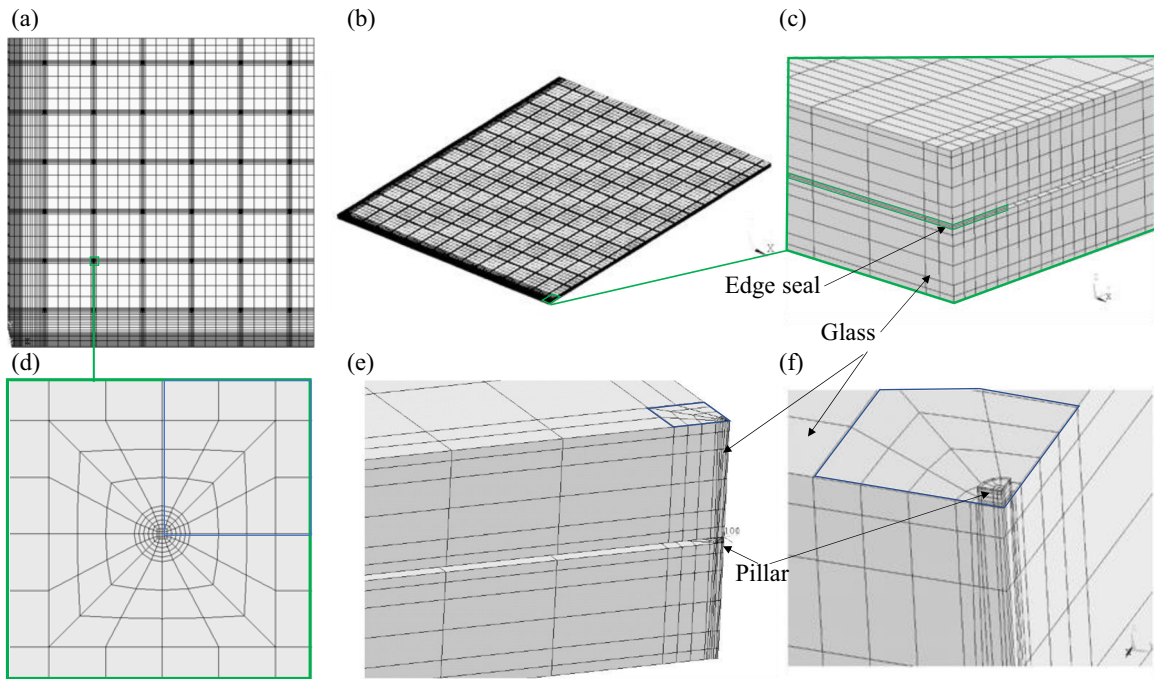
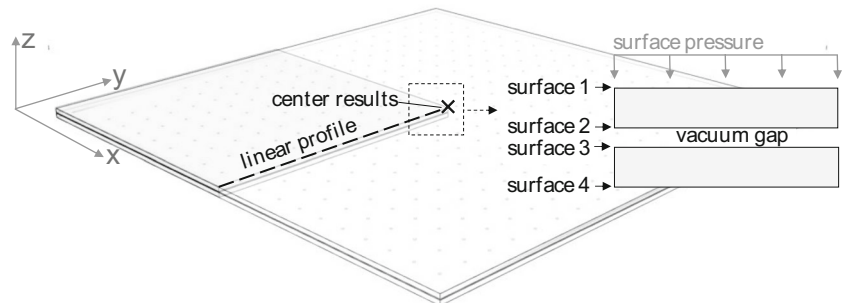


Fig. 3 Illustration of the different mesh regions of the glass in the VIG FEM; **a** whole quarter model (surface plot), **b** whole quarter model (3D), **c** local mesh at the edge, **d** the local mesh over a single pillar (surface plot), **e** local cut section of glass-pillar-glass area, **f** local pillar mesh

Fig. 4 An illustration of the FEM quarter model with wind load orientation and, surface and profile locations highlighted



demonstrated in previous work by Chiu (2015). It is important to note that the clamping of the glass edge results in greater strain of the glass, and BC 2 represents the extreme limit of the edge stress to be expected in a VIG under such a condition. In the solution phase, atmospheric pressure on the glass was solved as the first load step, followed by the wind load as a surface pressure in the second load step.

Clearly, there are various designs of the VIG, in particular, as currently available commercial products. It is beyond the scope of this work to consider the performance of all available configurations. Therefore, here the performance of the VIG was characterized

with respect to a reference configuration. The material properties and the design parameters of the reference case are summarized in Tables 1 and 2. The surface stress on the glass is dependent on the pillar separation since atmospheric pressure will deform the unsupported glass between pillars (compare Fig. 2) and between the edge seal and the first row of pillars. Therefore, to limit the areas of unsupported glass, the edge-to-pillar separation in the model was always set to be equal to the pillar-to-pillar separation, or less. The reference case is a VIG with an air-to-air, centre-of-glazing, U-value of $0.45 \text{ Wm}^{-2} \text{ K}^{-1}$ (calculated using the design methods provided in Turner et al. (1994).

Table 1 Properties of the materials used in the FEM

	Density ρ (kg/m ³)	Young's modulus (MPa)	Poisson's ratio (—)
Soda lime glass	2500	70,000	0.21
Solder glass	2500	70,000	0.22
Pillars	7850	210,000	0.3

Table 2 Geometric design values used in the FEM for the reference case

Glass thickness	4 mm
Pillar separation	40 mm
Pillar height	0.2 mm
Pillar diameter	0.5 mm
Edge seal width	6 mm

5 Results and discussion

In the presented results, the label "glass thickness $t = 4$ mm" refers to a VIG consisting of two 4 mm thick glass sheets. For comparison to a monolithic glass pane, the thickness of the monolithic pane is equivalent to the two panes of the VIG. Thus, in this case, $t = 4$ mm corresponds to a monolithic pane that is 8 mm thick. Both atmospheric pressure and wind load were applied in the FEM simulations, and Fig. 5 are the surface plots for both load steps from the FEM. The left plot shows atmospheric pressure only, while the right plot shows atmospheric pressure plus wind. The plots display the deflection in the z -direction (normal to the glass surface) as well as the first principal stress distribution on Surface 1 and 4 as defined in Fig. 4. From the absolute values, it is clear that adding the wind load significantly changes the total deformation, while the maximum stress is still highly dependent on atmospheric pressure, as shown by the line plots above a row of pillar. To highlight the effects of wind load and eliminate the periodic and localized stress field due to the pillars, in the subsequent discussion (unless otherwise specified) the data are for wind load only (i.e., atmospheric pressure was subtracted). It is reasonable to suggest that a VIG exhibits "direct shear coupling" between

the glass panes due to the rigid edge seal and the combination of the pillar array and applied atmospheric pressure. Therefore, in the following, we compare the VIG to an equivalent thickness monolithic pane, which could enable the application of existing plate theory to calculate the VIG's mechanical behaviour. In this work, we also employed an analytical solution derived from high-order shear deformation theory suggested by Adim et al. (2016). Differences in the results are discussed below.

The external surface stress field on the glass in a VIG depends on various factors such as the glass thickness and size, the applied surface pressure, and the boundary condition at the edge of the unit. In Fig. 6, the deflection and surface stress at the centre of a VIG and a monolithic glass pane are shown for different glass sizes and thicknesses of 3 and 5 mm. These results were obtained from both FEM simulations and an analytical solution based on a high-order shear deformation theory. For a pane size below 800 mm, the results from the FEM simulations and analytical solution are in good agreement. However, for larger VIG units, non-linear bending can limit the deflection and resulting surface stresses. This non-linear behaviour was expected and has been observed in the thermo-mechanical load behaviour of VIGs in previous studies (Wullschleger et al. (2009); Aronen and Kocer 2017). In general, the agreement between the FEM and analytical solution is within 15%, as long as the non-linear plate bending limit is not exceeded.

Interestingly the simulation data of the VIG shows a higher stiffness as compared to the results of the simulated monolithic pane: Fig. 6 Out-of-Plane Centre Deflection and the Stress component σ_{yy} at the centre, as a function of glass size. Numerical and analytical results are plotted for a constant surface pressure of 2 kPa and glass thickness of 3 & 5 mm. Previous experimental studies conducted by others showed that the stiffness of the VIG is similar to that of an equivalent monolithic pane that has a thickness of about 85–95% of the total thickness of the VIG panes. However, our simulation results indicate that the stiffness of a VIG is higher than that of a simulated monolithic pane, particularly for larger sample sizes. The difference in stiffness between our results and those of previous experiments may be attributed to the fact that the previous studies used small-sized units, which may not have fully captured the effect of the coupling between the glass panes in larger VIG units.

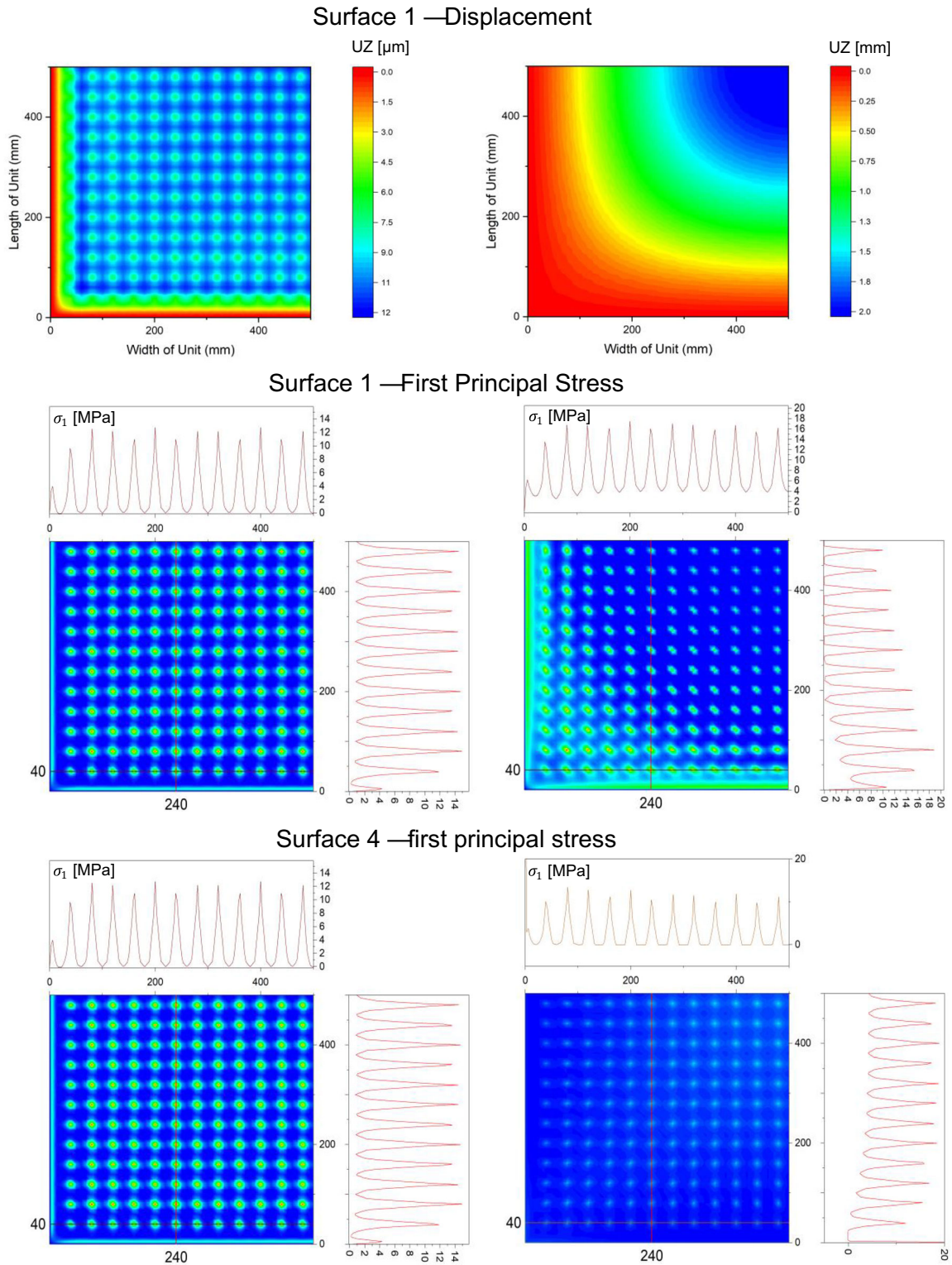


Fig. 5 FE surface plots, from left to right: atm pressure only, atmospheric pressure and wind, from top to bottom: plot of UZ displacement, plot of first principal stress on surface 1, plot of first principal stress on surface 4

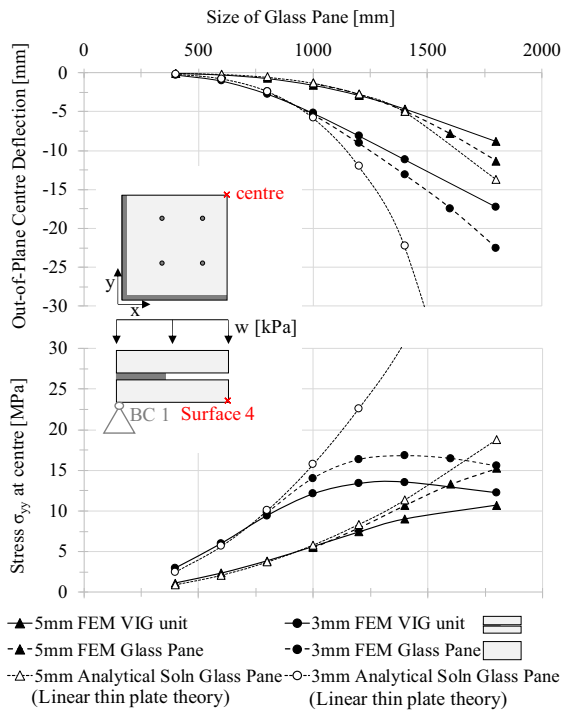


Fig. 6 Out-of-Plane Centre Deflection and the Stress component σ_{yy} (Which at the centre is equal to σ_{xx} and the first and second principal stress due to model and load symmetry) at the centre, as a function of glass size. Numerical and analytical results are plotted for a constant surface pressure of 2 kPa and glass thickness of 3 & 5 mm

The VIG consists of two glass panes that are coupled together through the rigid edge seal and the pillar array, as well as through atmospheric pressure acting on the glass. The results presented in Fig. 6 demonstrate that the increased stiffness of the VIG is due to this coupling between the glass panes, which limits their individual deformation when compared to a single pane of glass. However, the results also suggest that the VIG cannot be simply equated to a monolithic glass pane, unless the glass size is limited. In other words, for larger VIG units, the non-linear bending limits the deflection and resulting surface stresses, which means that the VIG behaves differently from a single pane of glass. Nevertheless, the FEM results suggest that assuming equivalence to a monolithic pane when predicting the potential mechanical behaviour of large VIG units is a conservative approach. Therefore, it's important to consider the coupling effect between the glass panes in the VIG when designing and analysing such units.

To understand the limits of the application of VIG with respect to wind loads, it is essential to accurately quantify the stress level and its distribution over the glass panes. Figure 7 presents plots of the primary Cartesian stress components σ_{xx} , σ_{yy} , and σ_{xy} for BC 1 and BC 2, for the outer glass surfaces 1 and 4, as shown in Fig. 4. The stress profile is over the line from the edge (midway between two corners) to the centre of the pane (Fig. 4), which is the line of mirror symmetry. For a surface pressure of 2 kPa, the highest magnitude of stress is either at the centre of the glass on surface 4 or at the edge of the glass on surface 1, with respect to BC 1 or BC 2, respectively. We expect that in a real frame, the boundary condition on the glass should be between BC 1 and BC 2. Therefore, the BC 2 result on surface 1 would be a good conservative maximum stress limit to consider for a VIG designed to withstand wind loads.

In Figs. 8 and 9, we plot the maximum surface stress over glass surface 1, for BC 2, with respect to glass size, thickness, and surface pressure magnitude. Figure 8 gives an overview of the influence of the parameters mentioned above on the stress portion due to the surface pressure only. For design purposes the stress distribution due to wind load and atmospheric pressure (depending on VIG design, i.e. on glass thickness and pillar separation, compare Fig. 2) always need to be considered in combination. As a conservative estimate maximum stress values can be combined using linear superposition. In Fig. 9 the hatched areas therefore represent the portion due to atmospheric pressure (exemplarily for a pillar separation of 40 mm). The red dotted lines in Fig. 9 represent the maximum allowable stress for AN glass according to ASTM E1300 (2016) and EN 16612:2019, highlighting the design options for VIG in relation to the Standards. Our results indicate that for AN glass, a thick glass pane (greater than 2×3 mm) is necessary for a pillar separation higher than 30 mm (see Fig. 2 also) and a unit size greater than 800 mm to ensure that the unit does not fail under a wind load of 2 kPa. It is important to remember that increasing glass thickness to gain mechanical advantage leads to increased thermal heat flow through the edge region due to the greater lateral heat flow observed through thick glass panes (Simko et al. 1995). Conversely, reducing pillar separation to decrease mechanical stress results in higher heat flow (Wilson et al. 1998). Therefore, the design of VIG is a compromise between desired mechanical and thermal performance.

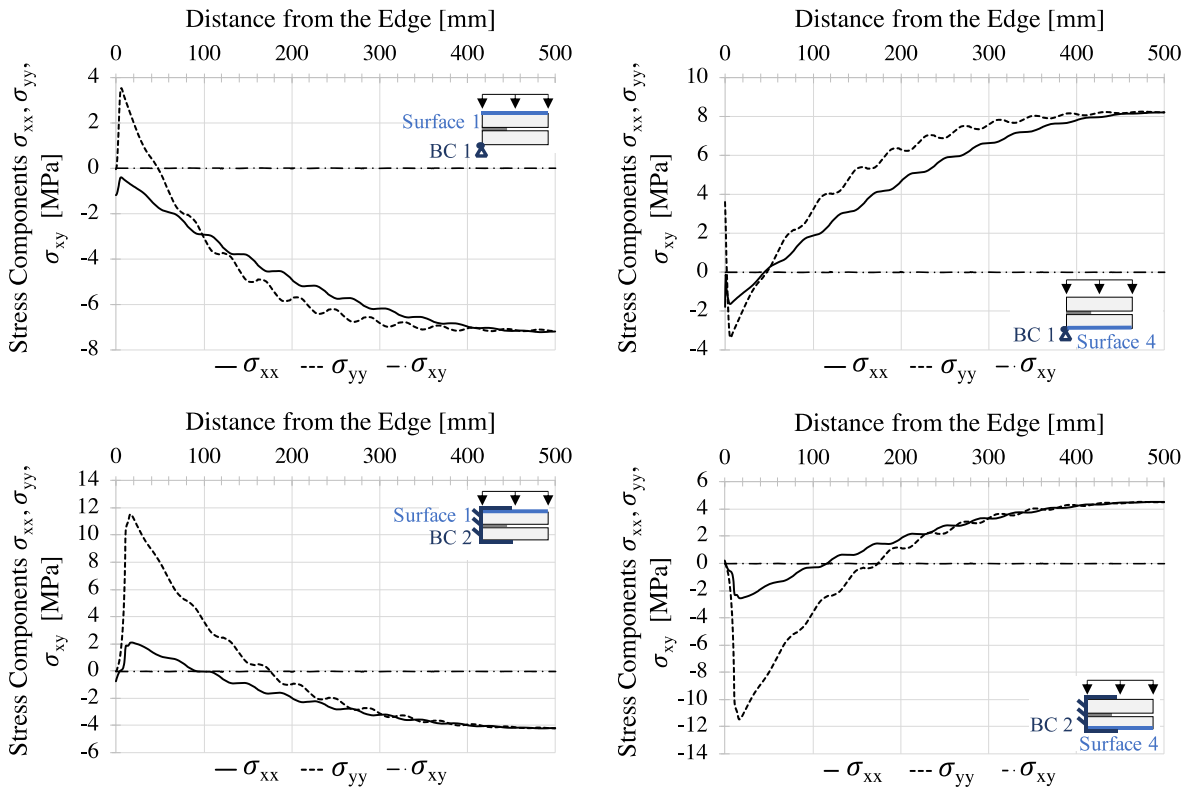


Fig. 7 Stress components σ_{xx} , σ_{yy} , and σ_{xy} , as a function of position over the glass surface. Each plot is for surface 1 and 4, and BC 1 and BC 2, for a glass size of 1000 mm, glass thickness of 4 mm and a surface pressure of 2kPa

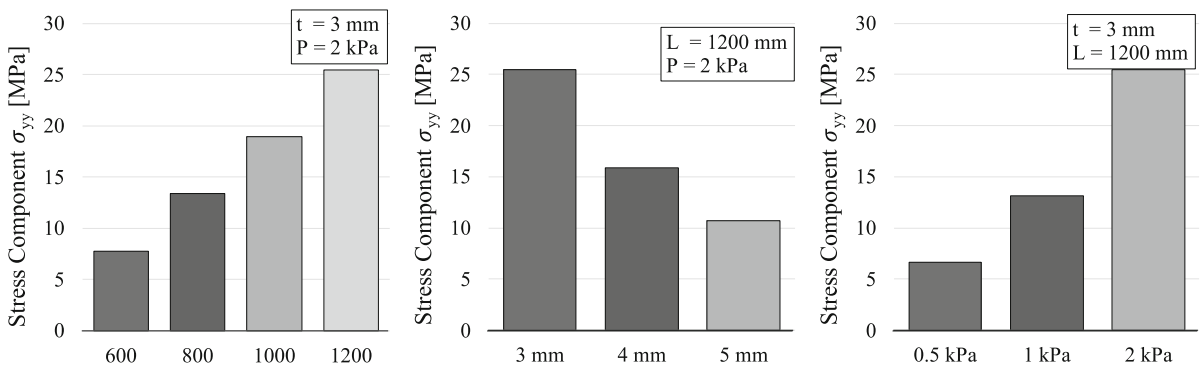


Fig. 8 Stress components σ_{yy} over the glass surface 1 and BC 2, with respect to unit size (left), glass thickness (centre) and magnitude of surface pressure (right)

The use of fully tempered glass would be advantageous. At this point it has to be noted that besides combined loading of wind load and atmospheric pressure, also atmospheric pressure alone can become critical in design as for AN the glass strength under permanent load is always smaller than the one considered in this study.

6 Conclusion and future work

In this work we undertook a parametric study using ANSYS 18.0, to highlight the influence of different design parameters on the mechanical behavior of a VIG exposed to a constant surface pressure, which typically is used to represent wind load, as outlined by

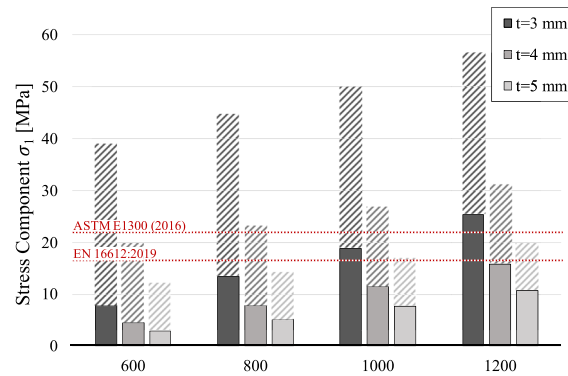


Fig. 9 The maximum tensile stress σ_1 (action side) over the glass surface 1 and for BC 2 and $P = 2$ kPa, with respect to unit size and variation of the thickness; Hatched areas represent the stress portion due to atmospheric pressure, exemplarily illustrated for a pillar separation of 40 mm; Maximum allowable stresses for AN glass according to ASTM E1300(2016) and EN 16612:2019 are given as dotted red lines (resistance side)

the European and North American Standards. The outcome of our stress analysis was placed in to context with respect to the glass design requirements as outlined in ASTM E1300 (2016) and EN 16612:2019. It was found that the Out-of-Plane Centre Deflection of the VIG was in good agreement with the FEM and analytical solutions of an equivalent thickness monolithic pane, for sample sizes below 800×800 mm. For larger glass sizes it was found that the VIG has a higher plate stiffness as compared to the equivalent thickness monolithic pane. The simulations also showed that the stresses in the glass panes are highly dependent on the edge of glass boundary condition. Further analysis of the non-trivial interaction between the glass panes, the pillars, the rigid edge seal and the constraint at the edge due to framing, is needed. This is future work, where strain measurements will be performed on VIG products exposed to a Standard wind load test. Even though the stresses produced on the internal vacuum side glass surfaces were not considered here, as a matter of completeness the pillar-glass contact needs to be described in greater detail. This can certainly be critical when considering cyclic loading of the VIG unit since wear, and thus, cumulative damage on the glass (over the pillar contact) should be investigated. Finally, with respect to the existing EU and North American Standards on wind load and glass design, the results presented in this paper showed that with appropriate design choices, the VIG can satisfy the requirements of Standards.

Acknowledgements The authors acknowledge the computing resources supporting this work, provided by the Sydney Informatics Hub, a Core Research Facility of the University of Sydney.

Funding Open Access funding enabled and organized by Projekt DEAL. Funding was provided by Bundesministerium für Wirtschaft und Energie (Grant No. 03EGB0021B).

Data Availability All data are stored on TU Darmstadt infrastructure with user management and regular backups. Access can be provided upon request.

Declarations

Conflict of interest On behalf of all authors, the corresponding author states that there is no conflict of interest.

Open Access This article is licensed under a Creative Commons Attribution 4.0 International License, which permits use, sharing, adaptation, distribution and reproduction in any medium or format, as long as you give appropriate credit to the original author(s) and the source, provide a link to the Creative Commons licence, and indicate if changes were made. The images or other third party material in this article are included in the article's Creative Commons licence, unless indicated otherwise in a credit line to the material. If material is not included in the article's Creative Commons licence and your intended use is not permitted by statutory regulation or exceeds the permitted use, you will need to obtain permission directly from the copyright holder. To view a copy of this licence, visit <http://creativecommons.org/licenses/by/4.0/>.

References

- Adim, B., Daouadji, T.H., Rabahi, A.: A simple higher order shear deformation theory for mechanical behavior of laminated composite plates. *Int. J. Adv. Struct. Eng. (IJASE)* 8(2), 103–117 (2016)

- Aronen, A., Kocer, C.: Vacuum insulated glazing under the influence of a thermal load. In: *All Eyes on Glass, Glass Processing Days, Finland, Glass Processing Days, Glaston, Finland*, vol. GPD2017, pp. 273–279 (2017)
- ASCE 7–16.: *Minimum Design Loads for Buildings and Other Structures*. Standard, American Society of Civil Engineers (2016)
- ASTM E1300 (2016) *Standard Practice for Determining Load Resistance of Glass in Buildings*
- Budd, S.M.: The mechanisms of chemical reaction between silicate glass and attacking agents. Part 1. Electrophilic and nucleophilic mechanisms of attack. *Phys Chem Glass* **2**, 111–114 (1961)
- Chiu, A.: *Mechanical behaviour of vacuum insulated glazing*. Thesis, University of Sydney, School of Physics, Sydney, Australia (2015)
- Collins, R.E., Fischer-Cripps, A.C.: Design of support pillar arrays in flat evacuated windows. *Aust. J. Phys.* **44**(5), 545–564 (1991)
- Collins, R.E., Robinson, S.J.: Evacuated glazing. *Sol. Energy* **47**(1), 27–38 (1991)
- Collins, R.E., et al.: Measurement of local heat flow in flat evacuated glazing. *Int. J. Heat Mass Transf.* **36**(10), 2553–2563 (1993)
- Collins, R. E., et al.: *Vacuum glazing: design options and performance capability*. In: *Glass in Buildings Conference*, Bath UK. vol. 221 (1999).
- EN 16612 (2019–12): *Glass in building—determination of the lateral load resistance of glass panes by calculation, german version*. Standard, DIN Deutsches Institut für Normung e. V
- EN 1991-1-4:2005/AC:2010 (E): *Eurocode 1: Actions on structures—part 1–4: General actions—wind actions*. Standard, European Committee for Standardization (CEN) (2010)
- Fang, Y., Eames, P.C., Norton, B.: Effect of glass thickness on the thermal performance of evacuated glazing. *Sol. Energy* **81**(3), 395–404 (2007)
- Fischer-Cripps, A.C., Collins, R.E.: The probability of Hertzian fracture. *J. Mater. Sci.* **29**, 2216–2230 (1994)
- Fischer-Cripps, A.C., Collins, R.E.: Architectural glazings: Design standards and failure models. *Build. Environ.* **30**(1), 29–40 (1995)
- Fischer-Cripps, A.C., et al.: Stresses and fracture probability in evacuated glazing. *Build. Environ.* **30**(1), 41–59 (1995)
- Gavanski, E., Kopp, G.A.: Glass breakage tests under fluctuating wind loads. *J. Archit. Eng.* **17**(1), 34–41 (2011)
- Griffith, A.A.: The phenomena of rupture and flow in solids. *Philos. Trans. R. Soc. London Ser. A, Contain. Pap. Math. Phys. Character* **221**, 163–198 (1921). <https://doi.org/10.1098/rsta.1921.0006>
- Holmes, J.D.: *Wind Loading of Structures*. CRC Press (2007)
- ISO 19916-1.: *International Organisation for Standardization, Glass in building—vacuum insulating glass part 1: basic specification of products and evaluation methods for thermal and sound insulating performance*. (2018).
- ISO 19916-3.: *International Organisation for Standardization, Glass in building—vacuum insulating glass part 3: test methods for evaluation of performance under temperature differences* (2021).
- Kocer, C.: *Finite Element Analysis of the Mechanical Deformations in a Vacuum Glazing*, *Glass Processing Days, Finland*, vol. GPD2011, pp 540–544 (2011)
- Kocer, C.: *A Discussion of Highly Insulating Windows*, *Glass Processing Days, Finland*, vol. GPD2013, pp. 447–450 (2013)
- Lee, W., Kang, J., Cho, S.W.: A new structure of vacuum insulation glazing for edge effect reduction: A parametric study. *Int. J. Precis. Eng. Manuf.* **19**, 447–452 (2018)
- Liu, X.G., Bao, Y.W.: Theoretical and experimental studies on strength and stiffness of vacuum glazing. *Key Eng. Mater.* **544**, 265–270 (2013)
- Meyland, M.J., Nielsen, J.H., Kocer, C.: Tensile behaviour of soda-lime-silica glass and the significance of load duration—a literature review. *J. Build. Eng.* **44**, 102966 (2021)
- Michalske, T.A., Freiman, S.W.: A molecular interpretation of stress corrosion in silica. *Nature* **295**(5849), 511–512 (1982)
- Michalske, T.A., Freiman, S.W.: A molecular mechanism for stress corrosion in vitreous silica. *J. Am. Ceram. Soc.* **66**(4), 284–288 (1983)
- Ng, N., Collins, R.E., So, L.: Characterization of the thermal insulating properties of vacuum glazing. *Mater. Sci. Eng. B* **138**(2), 128–134 (2007)
- Park, J., Myunghwan, Oh., Lee, C.: Thermal performance optimization and experimental evaluation of vacuum-glazed windows manufactured via the in-vacuum method. *Energies* **12**(19), 3634 (2019)
- Riedel, H., et al.: Automated quality control of vacuum insulated glazing by convolutional neural network image classification. *Autom. Constr.* **135**, 104144 (2022)
- Schneider, J., et al.: *Glasbau: Grundlagen, Berechnung Konstruktion*. Springer-Verlag (2016)
- Schulz, I., et al.: *Das mechanische Verhalten von Vakuumisoliertgläsern unter Windbelastung*. *Ce/papers* **5**(1), 308–321 (2022)
- Schulz, I., et al.: *Ein Verfahren zum Nachweis von thermisch vorgespannten Vakuumisoliertglas-Hybriden*. *Ce/Papers* (2023) in press in March (2023).
- Simko, Torn M., et al.: *Edge conduction in vacuum glazing*. No. LBL-36958; CONF-951215-7. Lawrence Berkeley National Lab. (LBNL), Berkeley, CA (1995)
- Turner, G. M., et al.: *Limits to performance of evacuated glazing*. In: *Optical Materials Technology for Energy Efficiency and Solar Energy Conversion XIII*, vol. 2255, SPIE (1994).
- Wilson, C.F., Simko, T.M., Collins, R.E.: Heat conduction through the support pillars in vacuum glazing. *Sol. Energy* **63**(6), 393–406 (1998)
- Wullschleger, L., Manz, H., Ghazi Wakili, K.: Finite element analysis of temperature-induced deflection of vacuum glazing. *Constr. Build. Mater.* **23**(3), 1378–1388 (2009)

Publisher's Note Springer Nature remains neutral with regard to jurisdictional claims in published maps and institutional affiliations.